Reports

Activity density at a continental scale: What drives invertebrate biomass moving across the soil surface?

Michael Kaspari [1,5] Michael D. Weiser [1] Katie E. Marshall,[2] Matthew Miller,[1] Cameron Siler,[1,3] and
Kirsten de Beurs[4]

[1]*Department of Biology, Geographical Ecology Group, University of Oklahoma, Norman, Oklahoma 73019 USA*
[2]*Department of Zoology, University of British Columbia, Vancouver, British Columbia V6T 1Z4 Canada*
[3]*Sam Noble Oklahoma Museum of Natural History, University of Oklahoma, Norman, Oklahoma 73072-7029 USA*
[4]*Department of Geography and Environmental Sustainability, University of Oklahoma, Norman, Oklahoma 73019 USA*

Abstract. Activity density (AD), the rate that an individual taxon or its biomass moves through the environment, is used both to monitor communities and quantify the potential for ecosystem work. The Abundance Velocity Hypothesis posited that AD increases with above-ground net primary productivity (ANPP) and is a unimodal function of temperature. Here we show that, at continental extents, increasing ANPP may have nonlinear effects on AD: increasing abundance, but decreasing velocity as accumulating vegetation interferes with movement. We use 5 yr of data from the NEON invertebrate pitfall trap arrays including 43 locations and four habitat types for a total of 77 habitat–site combinations to evaluate continental drivers of invertebrate AD. ANPP and temperature accounted for one-third to 92% of variation in AD. As predicted, AD was a unimodal function of temperature in forests and grasslands but increased linearly in open scrublands. ANPP yielded further nonlinear effects, generating unimodal AD curves in wetlands, and bimodal curves in forests. While all four habitats showed no AD trends over 5 yr of sampling, these nonlinearities suggest that trends in AD, often used to infer changes in insect abundance, will vary qualitatively across ecoregions.

Key words: activity density; biovolume; forests; geographical ecology; grasslands; invertebrates; monitoring; National Ecological Observatory Network; net primary productivity; scrublands; temperature; wetlands.

Introduction

Activity density (AD) is an often measured, if poorly understood, variable in community ecology (Kaspari and de Beurs 2019). Quantified by a variety of methods (e.g., baits, pitfall and camera traps; Southwood 1978, O'Connell and Nichols 2010, Gibb 2017), AD is the rate that organisms, as individuals or biomass, intersect a given point in space (e.g., the number of individuals captured by camera traps in a month, or the biomass of insects from a week's worth of bait or pitfall trapping events). A deep understanding of AD is important for at least two reasons. First, it approximates the rates of a variety of interesting phenomena, including the rate that

predators find their prey, herbivores find their host plants, and mutualists find each other. Second, AD is commonly used to monitor, and infer change or stasis in, insect abundance (Hallmann 2017, Gibb et al. 2019, Seibold 2019, Wagner et al. 2021).

In the Abundance-Velocity Hypothesis (Kaspari and de Beurs 2019), AD is decomposed into the product of a taxon's abundance and movement velocity. Both abundance and velocity have environmental drivers. As animals are made of carbon, the number/biomass of animals should ultimately be constrained by an ecosystem's plant productivity (g $C \cdot m^{-2} \cdot yr^{-1}$, Oksanen et al. 1981, Wright 1983). Aboveground net primary productivity (ANPP) predicts gradients of abundance in animals from ants (Kaspari and Alonso 2000) to ungulates (Pettorelli et al. 2009). Next, for a given abundance of animals, the more they move, they more likely they are to be captured in a trap. One axiom from Thermal Performance Theory is that velocity, like other metabolically constrained

Fig. 1. Annual activity density (AD, mL·trap^{-1}·yr^{-1}) reflects the biomass of individuals and their rate of movement through the ecosystem, but its drivers vary systematically with ecosystem type. Increasing aboveground net primary productivity (ANPP, white line) increases the ability for an ecosystem to build invertebrate biomass, but also increases shade and litter, thus decreasing two factors promoting velocity: surface temperature and permeability (black line).

behavior, is a unimodal function of temperature (Bennett 1990, Hurlbert and Ballantyne 2008, Angilletta 2009, Kaspari et al. 2016, Sinclair 2016, Prather et al. 2018). In the first geographic test of the Abundance-Velocity Hypothesis, ANPP accounted for 40% of the 19-fold variation in AD from the boreal to the tropics (Kaspari and de Beurs 2019). In an Australian desert, where ANPP is likely constrained by precipitation (Rosenzweig 1968), both precipitation and temperature contributed to the AD of ants (Gibb et al. 2019).

However, the ANPP prediction of the Abundance-Velocity Hypothesis may be complicated when tested across the variety of habitats present across a continental ecotone (Fig. 1). Despite increasing abundance, rising ANPP may decrease velocity given the decreased permeability of high ANPP habitats. For example, an ant crawling through a low-ANPP scrub or patchy short-grass prairie can move more easily than one scrambling through the thick thatch of a tallgrass prairie or a litter-strewn forest floor (Kaspari and Weiser 1999). Thus, the positive effect of ANPP on AD predicted by the Abundance-Velocity Hypothesis is likely further modified, and made nonlinear, by the opposing effects of increasing NPP on abundance and velocity.

Toward achieving a deeper understanding of the drivers of AD, we analyze invertebrate pitfall trap arrays at a continental scale from terrestrial sites of the National Ecological Observatory Network (NEON, Levan 2020). We evaluate the Abundance-Velocity Hypothesis across four primary habitat categories, measuring the movement of invertebrate biomass across the soil surface.

METHODS

We measured average annual activity density (AD, [mL of invertebrates]·trap^{-1}·yr^{-1}) from 43 terrestrial

sites of NEON (Appendix S1: Fig. S1). At each site, NEON runs 10 arrays of pitfall traps (four traps per array from 2015 to 2017, three henceforth; Levan 2020). A site's arrays were assigned one of 10 habitat types that we collapsed into four (forest, grassland, scrub, wetland, Appendix S1: Section S1), and measured AD for two of each of 77 site-habitats for each available year.

Pitfall traps as samples of activity density

NEON collects and stores pitfall trap samples in 95% EtOH at 14-d intervals across each site's growing season (protocols summarized in Levan [2020], and Appendix S1: Methods S1). Growing season begin and end dates correspond to that interval when average minimum temperatures exceeded 4°C for 10 d. A single 14-d event's AD was read as the invertebrate volume (mL) in a storage tube (Appendix S1: Fig. S2); such measures were highly repeatable ($r^2 = 0.99$, Appendix S1: Fig. S3). We measure annual AD of a site-habitat as the average of the summed annual catches for the two arrays, divided by the number of traps per array (four traps per array were sampled from 2015 to 2017, three traps henceforth, mL·trap^{-1}·yr^{-1}).

Measuring bioclimatic drivers

We estimated each site-habitat's average growing season temperature using the mean temperature of every two-week sampling period from the PRISM Climate Group (data *available online*).[6] These data summarize 10,000 minimum and maximum daily temperatures from weather stations in the contiguous 48 states as spatial grids at 4-km spatial resolution (Daly et al. 2008). We selected the mean temperature from Prism's 4 × 4 km

[6] http://prism.oregonstate.edu

grid value coinciding with each NEON trap array. Temperatures from sites in Alaska and Puerto Rico, not covered by PRISM, were estimated from local weather stations.

We estimated annual aboveground net primary productivity (ANPP, g C·m^{-2}·yr^{-1}) by first summing the site-habitat's actual evapotranspiration (AET, mm) across the growing season using the MODIS/Terra Net Evapotranspiration product MOD16A2 V6 providing the sum of ET for every 8-d period at 500-m spatial resolution. This MODIS product is based on the logic of the Penman-Monteith equation and combines both daily meteorological measures plus sensed observations (Running and Mu 2017). We then used a modified version of Rosenzweig's (1968) regression to convert annual AET into measures of aboveground productivity (Kaspari 2000).

Using imaging to examine how invertebrate size and number determine volume

For a subset of the data from 2016, we decomposed AD into number of individuals and their median size. We used three trap catches, from the first, middle, and last of a site's 2016 growing season from 49 site-habitats yielding a total of 179 samples (some samples could not be processed when the lab was shut due to COVID-19 restrictions). Invertebrates in each sample were distributed evenly by forceps on a white ceramic plate and photographed at a resolution of 729 pixels/mm^2. We used the *Analyze Particles* command in the Fiji implementation of ImageJ (Schneider and Rasband 2012), to count the number of individuals and the median area of each individual (mm^2) per sample. To get a rough comparison of the composition of each of the four habitats, we classified each image into one of 30 taxonomic categories (see Appendix S1: Section S1 for further detail).

Statistics

To better characterize the structure and dynamics of AD, we first explored how our metric (i.e., mL) arises from the number of individuals and their median size. For that, we used simple OLS regression via the lm function in R v.3.5.3 (R Core Team 2020). Similarly, for each site-habitat, we tested for 5-yr trends in AD 2015–2019. Finally, we contrasted the composition of the four habitats by collapsing variation in AD among the eight most common taxa with a Principal Component Analysis, then contrasting the loadings of PC1 and PC2 across the four focal habitat categories.

Next, we analysed how a site-habitat's average annual AD covaries with its average annual ANPP and temperature as predicted by the Abundance-Velocity hypothesis. We log$_{10}$-transformed ANPP and AD as they varied 1,000- and 100-fold, respectively. For both ANPP and growing season temperature, we used linear and cubic regressions to test for nonlinearity in AD response. We used the MuMIn package (Bartoń 2018) in R to identify all possible models with a $\Delta AIC_c < 2$ (difference between a given model and the best model of the Akaike information criterion corrected for sample size, Burnham and Anderson 2002).

RESULTS

Activity density (AD) of individual trapping events (mL·trap^{-1}·14 d^{-1}) increased with both the number and size of individuals in a trap array sample (Appendix S1: Fig. S4). Both varied 100-fold (19–2,855 individuals, 0.30–69 mm^2 respectively, $n = 179$). The number of individuals in the trap accounted for 43% of the variation in AD (AD $= 0.63 \times$ abundance$^{0.62}$, $P < 0.001$). Median size when added to the first linear model accounted for an additional 7% of the variation (AD $= 16.4 \times$ size$^{0.19}$, $P < 0.001$). Therefore, about one-half of the variation in AD could be accounted for by positive decelerating functions of both invertebrate number and size, which among themselves had a weak negative correlation (individuals $= 2.9 \times$ size$^{-0.16}$, $r^2 = 0.02$, $P = 0.049$, Appendix S1: Fig. S4).

The taxonomic composition of pitfall arrays varied with habitat type (Appendix S1: Fig. S5). Hymenoptera outnumbered all other taxa in pitfalls from grasslands and scrub, with the number of the other six dominant taxa more evenly distributed in forests and wetlands. Using Principal Components analysis, PC1 (Hymenoptera loading $= 0.998$) reflected this difference (Wilcoxon $\chi^2_{41,3} = 11.5$, $P = 0.0092$), while PC2 and PC3 did not differ.

Using all data from 2015–2019 (for what will ultimately be a 30-yr data set, Levan 2020) an OLS regression revealed no 5-yr trends in AD for any of the four habitats (Appendix S1: Fig. S6, all four regressions had $P > 0.16$ and $r^2 < 0.05$).

Using abundance velocity to explore the continental geography of activity density

Mean annual AD varied 43-fold across the site-habitats (from 3.7 mL·trap^{-1}·yr^{-1} in an Alaskan Taiga to 160.0 mL·trap^{-1}·yr^{-1} in Arizona scrub). Using AIC$_c$ informed least squares regression, each habitat yielded a different best model from the Abundance-Velocity Hypothesis (Fig. 2, Appendix S1: Table S1). For forests, four models accounted for about one-third of observed variation in AD. All shared a U-shaped relationship with ANPP (i.e., a negative ANPP and positive ANPP^3 term), and three added positive/negative effects of temperature. Grasslands yielded one best model: a positive decelerating relationship with temperature accounting for 71% of variation in AD. Scrublands yielded two models describing an increasing function of temperature accounting for about one-half of the variation in AD. Wetlands yielded one best model describing a unimodal relationship with ANPP that accounted for 92% of variation in AD.
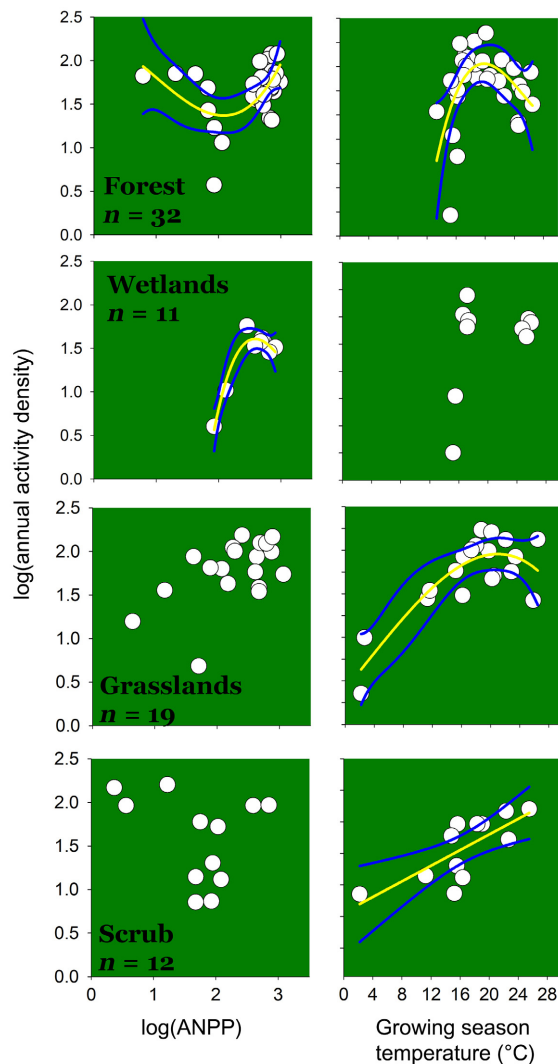
Reports

FIG. 2. The average annual activity density of four habitat types as a function of two drivers from the Abundance Velocity Hypothesis. Activity density ($mL \cdot trap^{-1} \, yr^{-1}$) responds to ANPP ($g \, C \cdot m^{-2} \, yr^{-1}$) and environmental temperature in different ways depending on habitat. Values are means. Yellow lines show best fit regression; blue lines show 95% confidence intervals.

DISCUSSION

Networks of traps that measure activity density are key parts of a strategy to quantify ecosystem responses to global heating, habitat conversion, and CO_2 fertilization (Cardoso 2020). Here we use an important new data set, the NEON continental pitfall network, to test predictions from the Abundance-Velocity Hypothesis. The model works well in revealing the role of temperature on AD from the Arctic to the subtropics: three of four habitat categories yielded the predicted positive or unimodal change in AD with temperature. Activity density, an ecosystem phenomenon, recapitulates the unimodal curves axiomatic for individuals in Thermal

Performance Theory (Angilletta 2009, Huey and King-solver 2019). However, AD did not increase monotonically with ANPP as predicted by Kaspari and de Beurs (2019), but was either insensitive to ANPP or was a unimodal or a concave-upward function of ecosystem productivity. These habitat-specific nonlinearities in AD are of particular interest given its widespread use, from malaise traps (Hallmann et al. 2017, 2020), windowpane traps (Seibold et al. 2019), camera traps (Steenweg 2017), and pitfall traps (Gibb et al. 2019), in searching for temporal trends in Anthropocene insect populations. For example, given each habitat's unique temperature–AD curve, a 4°C increase from a current mean of 20°C is predicted to generate decreases, no change, or increases in AD in North American forests, grasslands, and scrub-lands, respectively.

Temperature was a strong predictor of continental-scale variation in annual AD. The AD of scrub and grassland habitats both reveal monotonic limitation by temperature, with a clear diminishing effect in the warm-est grasslands. That a single driver like temperature can account for one-half to three-quarters of the variation in a basic ecosystem property like AD is an important clue for understanding how ecosystem services driven by invertebrates may change with temperature. However, temperature effects were weaker in wetlands and forests. One reason for this discrepancy may be the buffered microclimates experienced in both of these major habitat types: for the same solar energy, invertebrates in the still, shaded air of the forest floor, for example, live in a cooler environment with fewer temperature extremes (Kaspari et al. 2015, De Frenne et al. 2019).

Another, perhaps complimentary, hypothesis is that Hymenoptera, mainly ants, dominate AD in grasslands and scrublands compared to the more equitable distribution of invertebrates in forest and wetlands (Appendix S1: Fig. S5). Most ants, compared to many other invertebrates like fruit flies (Rosenberg and Blad 1983) are notoriously thermophilic, with thermal maxima well above 40°C (Kaspari et al. 2015, Stark et al. 2017, Bujan et al. 2020). In ant-dominated communities, higher temperatures may drive still higher AD's even in the warmest ecosystems. The exception that tests the rule comes from ant genera with relatively low thermal toler-ances, and that live in the detritus of the forest floor, which are declining in abundance relative to those with higher tolerances (Roeder et al. 2021). This suggests that many current ambiguities in interpreting bulk-based measures of AD (Hallmann et al. 2017, 2020, Seibold et al. 2019) will be clarified when the challenges of automating taxonomic identification are solved (e.g., Blair et al. 2020).

The variety of AD–ANPP curves across the four habi-tats (Fig. 2) also points to the importance of the plants and their architecture in predicting the future of AD from scrublands to forests. Invertebrate communities decrease AD as ANPP increases from the sparse desert pine forests of Moab Utah but increase again beyond

Reports

ANPP of 100 g C·m^{-2}·yr^{-1}. Such values of ~100 also generate AD minima in the three other habitats as well. We posit that the lack of a monotonic increasing ANPP–AD curve does not reflect the failure of ANPP in regulating a site's invertebrate abundance. Quadrat methods that count individuals and remove movement effects show a strong effect of ANPP in promoting the abundance of ants (Kaspari et al. 2000).

Instead, our working hypothesis on the dual role of ANPP lies in its opposing roles in (1) generating animal biomass and (2) decreasing the permeability of the habitat and thus impeding invertebrate velocity (Fig. 1). Moving up the North American ANPP gradient accumulates plant and litter debris along the way. This in turn increasingly hinders invertebrate movement until further increases in ANPP, and the commensurate boost in invertebrate abundance and biomass, counters this effect. In our earlier test of the Abundance Velocity Hypothesis, AD was always measured, from boreal to rainforest, on branches. There was no confounding effect of trap substrate on velocity (Kaspari and de Beurs 2019) as we find when traps are on the soil surface. In that 2019 study, ANPP accounted for 40% of global variation in AD. Future analyses of AD may thus benefit from an explicit consideration of how the physical structure of the environment interacts with the trap method. We predict, for example, that methods that quantify the AD of flying insects like malaise traps (Welti et al. 2021) and radar (Stepanian et al. 2020) will generate more uniform responses to temperature and ANPP across the variety of habitats and biomes of a continental study. As ecologists work to detect and diagnose large scales changes in invertebrate abundance, such details matter (Welti et al. 2021).

Literature Cited

Angilletta, M. J. 2009. Thermal adaptation: a theoretical and empirical synthesis. Oxford University Press, Oxford, UK.

Bartoń, K. 2018. Package 'MuMIn'. Model selection and model averaging based on information criteria (AICc and alike). R package. https://cran.r-project.org/web/packages/MuMIn/index.html

Bennett, A. 1990. Thermal dependence of locomotor capacity. American Journal of Physiology—Regulatory, Integrative and Comparative Physiology 259:253–258.

Blair, J., M. D. Weiser, M. Kaspari, M. Miller, C. Siler, and K. E. Marshall. 2020. Robust and simplified machine learning identification of pitfall trap-collected ground beetles at the continental scale. Ecology and Evolution 10:13143–13153.

Bujan, J., K. A. Roeder, K. de Beurs, M. D. Weiser, and M. Kaspari. 2020. Thermal diversity of North American ant communities: Cold tolerance but not heat tolerance tracks ecosystem temperature. Global Ecology and Biogeography 29:1486–1494.

Burnham, K. P., and D. R. Anderson. 2002. Model selection and multimodel inference: a practical information-theoretical approach. Springer, New York, New York, USA.

Cardoso, P., et al. 2020. Scientists' warning to humanity on insect extinctions. Biological Conservation 242:108426.

Daly, C., M. Halbleib, J. I. Smith, W. P. Gibson, M. K. Doggett, G. H. Taylor, J. Curtis, and P. P. Pasteris. 2008. Physiographically sensitive mapping of climatological temperature and precipitation across the conterminous United States. International Journal of Climatology: a Journal of the Royal Meteorological Society 28:2031–2064.

De Frenne, P., F. Zellweger, F. Rodríguez-Sánchez, B. R. Scheffers, K. Hylander, M. Luoto, M. Vellend, K. Verheyen, and J. Lenoir. 2019. Global buffering of temperatures under forest canopies. Nature Ecology & Evolution 3:744–749.

Gibb, H., et al. 2017. A global database of ant species abundances. Ecology 98:883–884.

Gibb, H., B. F. Grossman, C. R. Dickman, O. Decker, and G. M. Wardle. 2019. Long-term responses of desert ant assemblages to climate. Journal of Animal Ecology 88:1549–1563.

Hallmann, C. A., et al. 2017. More than 75 percent decline over 27 years in total flying insect biomass in protected areas. PLoS ONE 12:e0185809.

Hallmann, C. A., T. Zeegers, R. van Klink, R. Vermeulen, P. van Wielink, H. Spijkers, J. van Deijk, W. van Steenis, and E. Jongejans. 2020. Declining abundance of beetles, moths and caddisflies in the Netherlands. Insect Conservation and Diversity 13:127–139.

Huey, R. B., and J. G. Kingsolver. 2019. Climate warming, resource availability, and the metabolic meltdown of ectotherms. American Naturalist 194:E140–E150.

Hurlbert, A. H., F. IV Ballantyne, and S. Powell. 2008. Shaking a leg and hot to trot: the effects of body size and temperature on running speed in ants. Ecological Entomology 33:144–154.

Kaspari, M. 2021. The geography of activity density. Open Science Framework, data set. https://doi.org/10.17605/OSF.IO/F29KG

Kaspari, M., L. Alonso, and S. O'Donnell. 2000. Three energy variables predict ant abundance at a geographic scale. Proceedings of the Royal Society B 267:485–490.

Kaspari, M., N. A. Clay, J. Lucas, S. Revzen, A. Kay, and S. P. Yanoviak. 2016. Thermal adaptation and phosphorus shape thermal performance in an assemblage of rainforest ants. Ecology 97:1038–1047.

Kaspari, M., N. A. Clay, J. Lucas, S. P. Yanoviak, and A. Kay. 2015. Thermal adaptation generates a diversity of thermal limits in a rainforest ant community. Global Change Biology 21:1092–1102.

Kaspari, M., and K. de Beurs. 2019. On the geography of activity: productivity but not temperature constrains discovery rates by ectotherm consumers. Ecosphere 10:e02536.

Kaspari, M., and M. Weiser. 1999. The size-grain hypothesis and interspecific scaling in ants. Functional Ecology 13:530–538.

Levan, K. 2020. NEON user guide to ground beetle sampled from pitfall traps. NEON, Boulder, Colorado, USA.

O'Connell, A. F., J. D. Nichols, and K. U. Karanth. 2010. Camera traps in animal ecology: methods and analyses. Springer Science & Business Media, New York, New York, USA.

Oksanen, L., S. D. Fretwell, J. Arruda, and P. Niemela. 1981. Exploitation ecosystems in gradients of primary productivity. American Naturalist 118:240–262.

Pettorelli, N., J. Bro-Jørgensen, S. M. Durant, T. Blackburn, and C. Carbone. 2009. Energy availability and density estimates in African ungulates. American Naturalist 173:698–704.

Reports

Prather, R. M., K. A. Roeder, N. J. Sanders, and M. Kaspari. 2018. Using metabolic and thermal ecology to predict temperature dependent ecosystem activity: a test with prairie ants. Ecology 99:2113–2121.

R Core Team. 2020. R: A language and environment for statistical computing. R Foundation for Statistical Computing, Vienna, Austria. www.R-project.org

Roeder, K. A., J. Bujan, K. M. de Beurs, M. D. Weiser, and M. Kaspari. 2021. Thermal traits predict the winners and losers under climate change: an example from North American ant communities. Ecosphere 12:e03645.

Rosenberg, N., B. Blad, and S. Verma. 1983. Microclimate: the biological environment. Wiley and Sons, New York, New York, USA.

Rosenzweig, M. 1968. Net primary productivity of terrestrial environments: predictions from climatological data. American Naturalist 102:67–74.

Running, S., Q. Mu, and M. Zhao. 2017. MOD16A2 MODIS/ Terra Net Evapotranspiration 8-Day L4 Global 500m SIN Grid V006. Land Processes Distributed Active Archive Center (LP DAAC), U.S. Geological Survey, South Falls, South Dakota, USA.

Schneider, C. A., W. S. Rasband, and K. W. Eliceiri. 2012. NIH Image to ImageJ: 25 years of image analysis. Nature Methods 9:671–675.

Seibold, S., et al. 2019. Arthropod decline in grasslands and forests is associated with landscape-level drivers. Nature 574:671–674.

Sinclair, B. J., et al. 2016. Can we predict ectotherm responses to climate change using thermal performance curves and body temperatures? Ecology Letters 19:1372–1385.

Southwood, T. R. E. 1978. Ecological Methods. Second edition. Chapman and Hall, London, UK.

Stark, A. Y., B. J. Adams, J. L. Fredley, and S. P. Yanoviak. 2017. Out on a limb: thermal microenvironments in the tropical forest canopy and their relevance to ants. Journal of Thermal Biology 69:32–38.

Steenweg, R., et al. 2017. Scaling-up camera traps: Monitoring the planet's biodiversity with networks of remote sensors. Frontiers in Ecology and the Environment 15:26–34.

Stepanian, P. M., S. A. Entrekin, C. E. Wainwright, D. Mirkovic, J. L. Tank, and J. F. Kelly. 2020. Declines in an abundant aquatic insect, the burrowing mayfly, across major North American waterways. Proceedings of the National Academy of Sciences USA 117:2987–2992.

Wagner, D. L., E. M. Grames, M. L. Forister, M. R. Berenbaum, and D. Stopak. 2021. Insect decline in the Anthropocene: Death by a thousand cuts. Proceedings of the National Academy of Sciences USA 118(2):e2023989118.

Welti, E. A., A. Joern, A. M. Ellison, D. C. Lightfoot, S. Record, N. Rodenhouse, E. H. Stanley, and M. Kaspari. 2021. Studies of insect temporal trends must account for the complex sampling histories inherent to many long-term monitoring efforts. Nature Ecology and Evolution 5:589–591.

Wright, D. H. 1983. Species-energy theory: an extension of species-area theory. Oikos 41:496–506.

SUPPORTING INFORMATION

OPEN RESEARCH